Disposition and Metabolism of [^{14}C]Lemborexant in Healthy Human Subjects and Characterization of Its Circulating Metabolites [S]

 Takashi Ueno, Tomomi Ishida, Jagadeesh Aluri, Michiyuki Suzuki, Carsten T. Beuckmann, Takaaki Kameyama, Shoji Asakura, and Kazutomi Kusano

Eisai Co., Ltd., Ibaraki, Japan (T.U., T.I., C.T.B., T.K., S.A., K.K.); Eisai Inc., Woodcliff Lake, New Jersey (J.A.); and EA Pharma Co., Ltd., Tokyo, Japan (M.S.)

ABSTRACT

Lemborexant is a novel dual orexin receptor antagonist recently approved for the treatment of insomnia in the United States and Japan. Here, disposition and metabolic profiles were investigated in healthy human subjects. After single oral administration of 10 mg [^{14}C]lemborexant (100 μCi), plasma concentrations of lemborexant and radioactivity peaked at 1 hour postdose and decreased biphasically. Cumulative recovery of the administered radioactivity within 480 hours was 86.5% of the dose, with 29.1% in urine and 57.4% in feces. Unchanged lemborexant was not detected in urine but accounted for 13.0% of the dose in feces, suggesting that the main elimination pathway of lemborexant was metabolism. Metabolite analyses revealed that the major metabolic pathways of lemborexant are oxidation of the dimethylpyrimidine moiety and subsequent further oxidation and/or glucuronidation. In plasma, lemborexant was the dominant component, accounting for 26.5% of total drug-related exposure. M4, M9, M10, and M18 were detected as the major radioactive components; M10 was the only metabolite exceeding 10% of total drug-related exposure. Although M4, M9, and M10 showed binding affinity for orexin receptors comparable to that of lemborexant, their contributions to the sleep-promoting effects of lemborexant are likely low because of the limited brain penetration by P-glycoprotein. Exposure comparison between humans and nonclinical toxicology species confirmed that plasma exposure of M10 was higher in at least one animal species compared with that in humans, indicating that there is no disproportionate metabolite in humans, as defined by International Council for Harmonisation of Technical Requirements for Pharmaceuticals for Human Use M3(R2) and U.S. Food and Drug Administration Metabolite in Safety Testing guidance; therefore, no additional toxicology studies are needed.

SIGNIFICANCE STATEMENT

This study provides detailed data of the disposition and metabolism of lemborexant, a novel therapeutic drug for insomnia, in humans, as well as a characterization of the circulating metabolites and assessment of their contributions to efficacy and safety. The information presented herein furthers our understanding of the pharmacokinetic profiles of lemborexant and its metabolites and will promote the safe and effective use of lemborexant in the clinic.

Introduction

Insomnia is a common sleep disorder characterized by difficulties with falling asleep and/or maintaining sleep despite an adequate opportunity to sleep (Buysse, 2013). Patients suffering from insomnia usually report complaints of inadequate or poor-quality sleep, and the consequent sleep deprivation causes significant impairment in daytime performance. The prevalence of insomnia in the general adult population is estimated to be 12%–20% (Morin et al., 2011; Roth et al., 2011).

Orexin peptides are neuropeptides produced from the precursor prepro-orexin in orexin neurons located in the hypothalamus (de Lecea et al., 1998; Sakurai et al., 1998), and they are recognized as upstream regulators of neurotransmitters related to sleep and wakefulness. Orexin peptides bind to their receptors, orexin-1 receptor (OX1R) and orexin-2 receptor (OX2R) (Sakurai et al., 1998), and it has been reported that blockade of orexin receptors can promote sleep in animals and humans (Brisbare-Roch et al., 2007). Thus, the orexin signaling pathway has been studied as a promising drug target for insomnia.

Lemborexant (also called E2006 or Dayvigo) is a novel dual orexin receptor antagonist that shows high and selective binding affinities to human orexin receptors with rapid association and dissociation kinetics (Beuckmann et al., 2017). Preclinical in vivo assessments in rodents have shown that lemborexant exerts a sleep-promoting effect via the orexin signaling pathway (Beuckmann et al., 2019). In clinical studies, including two pivotal phase 3 studies, lemborexant improved sleep onset and sleep maintenance with minimal next-morning residual sleepiness and no significant impairment of next-morning driving performance in patients with insomnia (Murphy et al., 2017; Rosenberg et al., 2019; Vermeeren et al., 2019). Based on these and other data, lemborexant was approved for the treatment of insomnia by the U.S. Food and Drug Administration (FDA) in December 2019 and by the Ministry of Health, Labor and Welfare of Japan in January 2020. Lemborexant is also

ABBREVIATIONS: AMS, accelerator mass spectrometry; AUC, area under the concentration-time curve; AUC$_{(0-inf)}$, area under the concentration vs. time curve from time zero to infinity after administration; BCRP, breast cancer resistant protein; CFR, corrected flux ratio; DDI, drug-drug interaction; FDA, U.S. Food and Drug Administration; HPLC, high-performance liquid chromatography; LC-MS/MS, liquid chromatography-tandem mass spectrometry; LSC, liquid scintillation counting; m/z, mass-to-charge ratio; OX1R, orexin-1 receptor; OX2R, orexin-2 receptor; P$_{app}$, apparent permeability coefficient; P-gp, P-glycoprotein.

currently under clinical development for the treatment of irregular sleep-wake rhythm disorder.

Previously, we demonstrated in absorption, distribution, metabolism, and excretion studies with [14C]lemborexant in rats and monkeys that lemborexant was rapidly and completely absorbed after oral dosing and that the drug-derived radioactivity was excreted mainly into feces (Ueno et al., 2019). Furthermore, we found that lemborexant underwent extensive metabolism via diverse pathways in rats and monkeys, and various metabolites were detected in plasma and excreta (Ueno et al., 2019). Drug metabolites may be pharmacologically active, cause substantial drug-drug interactions (DDIs), or contribute to safety concerns; consequently, careful characterization of metabolites, including profiling of the major metabolites in plasma, is essential to ensure the safe use of therapeutics. The FDA Metabolite in Safety Testing and the International Council for Harmonization of Technical Requirements for Pharmaceuticals for Human Use M3(R2) guidance recommends confirming the relative exposure of circulating metabolites to total drug-related exposure in humans and the exposure coverage of circulating metabolites in nonclinical toxicology studies to evaluate the need for additional safety assessments of metabolites (ICH, 2010; FDA, 2020b). DDI guidance and guidelines issued by the FDA, European Medicine Agency, and Ministry of Health, Labor and Welfare of Japan use a metabolite-to-parent area under the concentration-time curve (AUC) ratio as the cutoff value for assessments of DDI potentials of metabolites (EMA, 2012; MHLW, 2019; FDA, 2020a). Thus, absorption, distribution, metabolism, and excretion studies are a crucial step during drug development to investigate the metabolic profiles of new chemical entities in humans and nonclinical toxicology species and provide detailed pharmacokinetic information not only of the parent drug but also of its metabolites, which is necessary to maximize the efficacy and safety of the drug.

The objectives of the present study were to investigate the disposition, mass balance, and metabolic profiles of [14C]lemborexant after oral administration in healthy human subjects. In vitro assessments were also conducted to evaluate possible contributions of circulating metabolites detected in human plasma to the sleep-promoting effect of lemborexant. In addition, exposure of the circulating metabolites were compared between humans and nonclinical toxicology species to ensure that safety assessments of the metabolites in nonclinical toxicology species would adequately evaluate safety in humans.

Materials and Methods

Chemicals and Reagents. Lemborexant and authentic metabolite standards were synthesized at Eisai Co., Ltd. (Ibaraki, Japan) or Eisai Inc. (Andover, MA). [14C]Lemborexant was synthesized at Ricerca Biosciences, LLC (Concord, OH), and its radiochemical purity and specific radioactivity were 97.5% and 4.02 mCi/mmol, respectively. The chemical structure of [14C]lemborexant is shown in Supplemental Fig. 1. Deuterium-labeled compounds used as internal standards were synthesized at Eisai Co., Ltd., or Shanghai ChemPartner Co., Ltd. (Shanghai, China). All other chemicals and reagents used were obtained from commercial suppliers.

Clinical Study. The clinical study was conducted at Covance Clinical Research Unit, Inc. (Madison, WI), in accordance with the Declaration of Helsinki. The study (E2006-A001-007; NCT02046213) was a single-radio-labeled-dose, open-label, single-center study and an absorption, metabolism, and excretion study. The study protocol, informed consent form, and appropriate related documents were approved by the institutional review board, and all subjects provided written informed consent prior to participation in the study. In the morning, after at least 10 hours of fasting overnight, eight healthy adult male subjects, aged 18–55 years old, received 10 mg of [14C]lemborexant containing 100 μCi as a single oral dose in capsule formulation. The subjects were confined to the study site for a minimum of 21 days and a maximum of 35 days. Urine, fecal, and toilet tissue samples were collected at 24-hour intervals, and collection

was continued until the combined excreta contained less than 1% of the administered radioactive dose at two consecutive 24-hour sample collection intervals, at which point the subjects were discharged from the study. Fecal and toilet tissue samples were mixed with water to prepare an approximate 20% (w/v) fecal homogenate and a suspension of toilet tissue, respectively. Blood samples were collected at the following time points: predose and 0.5, 1, 2, 3, 4, 6, 8, 12, 24, 48, 72, 96, 144, 216, 312, 408, 648, and 816 hours postdose; plasma samples were obtained by centrifugation of the blood samples.

Measurement of Total Radioactivity. Total radioactivity in plasma, urine, feces, and toilet tissue was measured by a combustion method. The samples were combusted using a model 307 Sample Oxidizer (Packard Instrument Company, Meriden, CT), and the resulting $^{14}CO_2$ was trapped in Carbo-Sorb and then mixed with PermaFluor (PerkinElmer, Waltham, MA). The radioactivity in the samples was measured by using liquid scintillation counters (models 2900TR and 2910TR; Packard Instrument Company) for at least 5 minutes or 100,000 counts. Oxidation efficiency was evaluated on each day of sample combustion by analyzing a commercial radiolabeled standard. All samples were analyzed in duplicate, when sample size allowed.

Quantitation of Concentrations in Plasma Samples by Liquid Chromatography-Tandem Mass Spectrometry. Preliminary assessments demonstrated that lemborexant metabolites M4, M9, and M10 showed relatively high plasma exposure in humans after oral administration of lemborexant. Therefore, plasma concentrations of not only lemborexant but also of these metabolites were measured by a validated liquid chromatography-tandem mass spectrometry (LC-MS/MS) method. Plasma samples (100 μl) were mixed with 25 μl of acetonitrile/distilled water (1:1, v/v) containing 0.1% formic acid and internal standards, and 100 μl of 10% ammonium hydroxide, and then methyl t-butyl ether (1 ml) was added for extraction of the analytes. Samples were centrifuged, and the organic solvent obtained as the supernatant was evaporated to dryness under a nitrogen gas stream and then reconstituted with 200 μl of acetonitrile/distilled water (1:1, v/v) containing 0.1% formic acid. The resultant aliquot was injected into a Shimadzu LS system coupled with a Sciex API-5000 mass spectrometer for LC-MS/MS analysis. The chromatographic separation was performed using a Phenomenex Kinetex XB-C18 column (5 μm, 250 × 4.6 mm) with high-performance liquid chromatography (HPLC) mobile phases of (A) 0.1% formic acid in water and (B) acetonitrile. Lemborexant, M4, M9, and M10, and the corresponding deuterium-labeled compounds used as internal standards, were identified based on their retention times and the mass units of the monitoring ions on the mass chromatograms. The multiple reaction monitoring transitions were mass-to-charge ratio (m/z) 411.2 → 287.0 for lemborexant; m/z 427.2 → 287.0 for M4, M9, and M10; m/z 414.2 → 290.1 for the internal standard of lemborexant; and m/z 430.2 → 290.2 for the internal standards of M4, M9, and M10. A calibration curve was obtained at a concentration range from 0.05 to 50 ng/ml by least-squares linear regression, with a weighting factor of $1/X^2$ on the ratio of the peak area of analytes to that of the corresponding internal standard against the nominal concentrations in the calibration standards.

Pharmacokinetic Calculation. Pharmacokinetic parameters were calculated from individual concentration-time profiles by noncompartmental analysis in Phoenix WinNonlin version 6.2 (Certara, St. Louis, MO).

Metabolite Profiling. Individual plasma samples from the eight subjects were mixed in equal volumes across subjects to prepare a single pooled plasma sample for each time point. The pooled plasma samples were further pooled across time points (0–96 hours postdose) according to the Hamilton pooling method to prepare an AUC-pooled plasma sample (Hamilton et al., 1981). Urine (0–120 hours postdose) and fecal homogenate samples (0–264 hours postdose) collected at the designated time intervals from each subject were pooled by combining volumes relative to the total volume or weight collected at the time interval. Plasma, urine, and fecal homogenate samples were each mixed with 3-fold volumes of methanol, shaken for 10 minutes, and centrifuged (1800g, 4°C, 10 minutes), and supernatants were collected. The resulting pellets were treated with the same volume of methanol once (for urine) or twice more (for plasma and fecal homogenates), and supernatants were combined and dried. The residue was reconstituted in N-methyl-2-pyrrolidinone/30% methanol (2:3, v/v) for plasma and fecal homogenates or 30% methanol for urine and centrifuged. The resulting supernatants were analyzed by HPLC and LC-MS/MS. Chromatographic separation was conducted using a previously reported method [HPLC condition 1 in Ueno et al. (2019)]. Radioactivity was detected by accelerator mass spectrometry (AMS) for plasma and by liquid scintillation counting (LSC) for

urine and feces. For the AMS analysis, HPLC eluate was fractionated every 30 seconds and pooled across the designated time points. AMS analysis was performed by using a Pelletron AMS system (1.5SDH-1 0.6MV; National Electrostatics Corporation, Tokyo, Japan) at Institute of Accelerator Analysis Ltd. (Kanagawa, Japan), as previously described (Tozuka et al., 2010), and the radioactivity concentration in the sample was calculated. For LSC analysis, HPLC eluate was fractionated every 18 seconds, and each HPLC fraction was mixed with Hionic-Fluor scintillator (PerkinElmer), after which LSC of radioactivity was conducted for 2 minutes. Radiochromatograms were constructed based on the radioactivity in each fraction determined by AMS or LSC. The proportion of parent or metabolites relative to total radioactivity in the sample (percentage of total radioactivity) was calculated based on the radiochromatogram and extraction recovery by methanol treatment. Since the AUC-pooled plasma sample prepared by the Hamilton pooling method was used for the analysis, the relative proportion (percentage of total radioactivity) corresponded to the proportion of each metabolite relative to total drug exposure (percentage of total drug-related exposure). The amount of parent or each metabolite in excreta relative to the radioactive dose (percentage of the dose) was also calculated by multiplying the proportion of parent or each metabolite in the sample (percentage of total radioactivity) by percent recovery of the radioactive dose excreted into urine or feces during the designated time periods.

Structural Analysis. Radioactivity in AUC-pooled plasma (0–96 hours postdose), urine (0–120 hours postdose), and fecal homogenate (0–264 hours postdose) samples was extracted by methanol, as described above, to obtain analytical samples. LC-MS/MS analyses were performed with an LTQ Orbitrap XL mass spectrometer (Thermo Fisher Scientific, Waltham, MA) as previously described (Ueno et al., 2019). Chemical structures of the metabolites were identified or elucidated based on mass spectra, retention times, exact mass, and molecular formula by comparing the authentic metabolite standards and glucuronide conjugates of hydroxylated metabolites that were generated by incubating each of the metabolites with human liver microsomes as previously described (Ueno et al., 2019). When the structure of a metabolite detected in the biologic samples was identified based on structural analysis, an M number (e.g., M1) was assigned to the metabolite. If the metabolite was identical to one previously reported (Ueno et al., 2019), the same M number was assigned.

In Vitro Measurement of Binding Affinity. The binding affinities of lemborexant metabolites (M4, M9, and M10) were measured by receptor binding assay using a 96-well FlashPlate (PerkinElmer) with a membrane suspension prepared from Chinese hamster ovary cells expressing human OX1R or OX2R, as previously described (Beuckmann et al., 2017). The membrane suspension was incubated with each metabolite at 0.6–600 nmol/L. Experiments were conducted three times in an identical fashion, and IC_{50} values were calculated for each experiment. Then, the final IC_{50} values and their SEMs were obtained by averaging the IC_{50} values from each experiment.

In Vitro P-Glycoprotein and Breast Cancer Resistant Protein Transport Assay. Transcellular transport of lemborexant and its metabolites (M4, M9, and M10) was assessed in LLC-PK1 cells and cells expressing human P-glycoprotein (P-gp; multidrug resistance protein 1) and in Madin-Darby Canine Kidney II cells and cells expressing human breast cancer resistant protein (BCRP), as previously described (Yoshida et al., 2014). The cells were individually seeded at densities of 6.0×10^5 cells/cm^2 for P-gp and 4.2×10^5 cells/cm^2 for BCRP onto the membrane filters of 24-well cell culture insert plates and cultured in a humidified, 5% CO_2/95% air atmosphere at 37°C for 6 days to prepare cell monolayers. Transcellular transport of lemborexant and its metabolites was evaluated at a concentration of 3 μmol/l in the absence or presence of verapamil (30 μmol/l), a typical P-gp inhibitor, or Ko143 (50 nmol/l), a typical BCRP inhibitor. The apparent permeability coefficient (P_{app}) in the basal-to-apical and the apical-to-basal directions, flux ratio, and corrected flux ratio (CFR) of lemborexant and its metabolites was calculated as previously described (Yoshida et al., 2014).

In Vitro Plasma Protein Binding Assay. Protein bindings of lemborexant, M4, M9, and M10 were determined in vitro using fresh human plasma obtained from healthy male volunteers by an equilibrium dialysis method as previously described (Yoshida et al., 2015). Plasma samples spiked with each test compound at concentrations of 100, 300, and 1000 ng/ml were dialyzed against PBS (pH 7.4) for 12 or 17 hours. Concentrations in the plasma and PBS samples were determined by LC-MS/MS, and plasma protein binding (%) was calculated as (1 – PBS concentration/plasma concentration) × 100.

Exposure Comparison of Circulating Metabolites between Humans and Animals. Plasma exposures of M4, M9, and M10 in humans and nonclinical toxicology species (i.e., rats and monkeys) were measured by validated LC-MS/MS methods using plasma samples obtained from a multiple-dose clinical study in humans and 4-week toxicokinetics studies in rats and monkeys. The clinical study (E2006-A001-003; NCT02039089) was a two-part, randomized, double-blind, placebo-controlled, multiple-dose study. In the second part of the study, six healthy Caucasian adult subjects received lemborexant at 10 mg once daily for 14 days. Plasma samples collected from healthy subjects at predose and at 0.5, 1, 1.5, 2, 3, 4, 5, 6, 8, 10, 12, and 24 hours postdose on day 14 were used for the assessment. In the 4-week toxicokinetics studies, lemborexant was orally administered once daily for 4 weeks to male and female Sprague-Dawley rats and cynomolgus monkeys at doses of 30, 100, and 1000 mg/kg for male rats and at doses of 10, 100, and 1000 mg/kg for female rats and male and female monkeys. Plasma samples collected from the animals at predose and at 0.5, 1, 2, 4, 8, and 24 hours postdose on day 28 were used. Plasma concentrations in the samples were measured by using the same validated method described in *Quantitation of Concentrations in Plasma Samples by Liquid Chromatography-Tandem Mass Spectrometry* or the method with minor modifications, and AUC values were determined by noncompartmental analysis and compared between humans and animals.

Results

Clinical Study. All eight subjects completed study E2006-A001-007, with the single dose of [^{14}C]lemborexant being well tolerated and no serious or drug-related adverse events reported. All reported adverse events were of mild severity, and there were no clinically significant changes in vital signs, clinical laboratory test results, or electrocardiogram measurements throughout the study period.
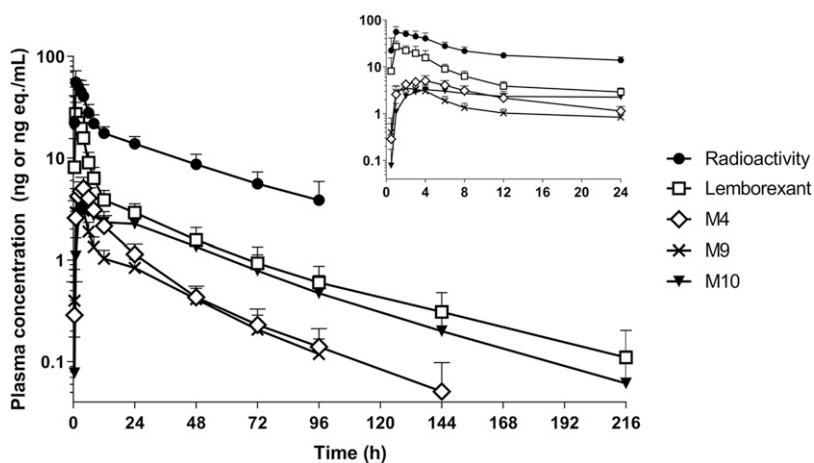

Fig. 1. Plasma concentration-time profiles of radioactivity, lemborexant, and its metabolites (M4, M9, and M10) after a single oral administration of [^{14}C]lemborexant at 10 mg (100 μCi) to healthy male subjects. Each point represents the mean + S.D. of eight subjects.

TABLE 1

Pharmacokinetic parameters of radioactivity, lemborexant, and its metabolites in plasma after a single oral administration of [^{14}C]lemborexant to healthy male volunteers

Parameters except for t_{max} represent the mean $\pm$ S.D. of eight subjects. The t_{max} is expressed as median and range.

Analyte	C_{max}	t_{max}	$AUC_{(0-inf)}$	$t_{1/2}$	CL/F	V_z/F	$AUC_{(0-inf)}$ Ratio
	ng/ml[a]	h	ng·h/ml[a]	h	l/h	l	% of radioactivity
Radioactivity	61.7 $\pm$ 9.81	1.00 (1.00–3.00)	1390 $\pm$ 450	43.6 $\pm$ 16.3	7.60 $\pm$ 2.12	440 $\pm$ 56.0	—
Lemborexant	29.5 $\pm$ 5.91	1.00 (1.00–3.00)	317 $\pm$ 92.5	45.2 $\pm$ 15.5	32.8 $\pm$ 7.79	2120 $\pm$ 907	23.1 $\pm$ 2.3
M4	5.18 $\pm$ 1.34	3.50 (2.00–4.00)	96.2 $\pm$ 27.1	30.5 $\pm$ 11.3	—	—	7.0 $\pm$ 0.8
M9	3.87 $\pm$ 0.533	2.00 (1.00–4.00)	65.6 $\pm$ 14.7	27.7 $\pm$ 6.21	—	—	4.9 $\pm$ 0.6
M10	3.32 $\pm$ 0.915	4.00 (3.00–8.00)	167 $\pm$ 57.4	36.2 $\pm$ 9.39	—	—	12.1 $\pm$ 2.5

—, not applicable; CL/F, oral clearance; $t_{1/2}$, terminal elimination half-life; t_{max}, time to reach maximum concentration; V_z/F, volume of distribution based on the terminal phase.

[a]Units for radioactivity are nanogram equivalent per milliliter and nanogram equivalent·hour per milliliter.

Pharmacokinetic Assessments. Plasma concentration-time profiles and pharmacokinetic parameters of radioactivity, lemborexant, and its metabolites (M4, M9, and M10) after a single oral administration of [^{14}C] lemborexant (10 mg) are shown in Fig. 1 and Table 1, respectively. Plasma concentration of radioactivity and lemborexant both peaked at 1 hour postdose and declined biphasically with terminal elimination half-lives of 43.6 and 45.2 hours, respectively. Oral clearance of radioactivity and lemborexant was 7.60 and 32.8 l/h, respectively. The metabolites, M4, M9, and M10, showed maximum concentrations at 2–4 hours postdose, and their terminal elimination half-lives (27.7–36.2 hours) were somewhat shorter than those of radioactivity and lemborexant.

Excretion of Radioactivity. After the single oral administration of [^{14}C]lemborexant, 86.5% of the administered radioactivity was recovered in excreta within 20 days, with individual subject values ranging from 75.6% to 91.7% (Fig. 2). The predominant route of excretion of the administered radioactivity was fecal excretion (57.4% of the dose). Urinary excretion accounted for 29.1% of the dose. The cumulative recovery of the administered radioactivity in toilet tissue was minimal (0.08% of the dose, data not shown).

Metabolite Profiling in Plasma and Excreta. The relative amounts of metabolites detected in plasma and excreta are summarized in Tables 2 and 3, respectively. Representative HPLC radiochromatograms for biologic samples are shown in Supplemental Fig. 2. Lemborexant was the dominant radioactive component in the AUC-pooled plasma sample, accounting for 26.5% of total drug-related exposure. M10, M9, M4, and M18 (glucuronide of M3) accounted for 12.5%, 6.6%, 6.3%, and 6.0% of total drug-related exposure, respectively. Each of the other metabolites accounted for 3.2% or less of total drug-related exposure.

In urine, M18 was the most dominant radioactive component, accounting for 11.0% of the dose. Met24 (a mixture of M12 and M4), Met9 [a mixture of M16 (glucuronide of M1), Met9-2, Met9-3, and M22 (glucuronide of M11)], and M21 (glucuronide of M9) accounted for 4.0%, 1.7%, and 1.4% of the dose, respectively. Each of the other metabolites accounted for less than 1.0% of the dose.

In feces, a mixture of lemborexant and Met29 accounted for 13.0% of the dose. In the LC-MS/MS analysis using the same sample, the mass intensity of lemborexant was much higher than that of Met29 (lemborexant vs. Met29 = 246,964,160 vs. 2,938,070), suggesting that the radioactivity of the mixture was mainly attributed to lemborexant. M12 was the prominent metabolite, accounting for 12.0% of the dose. Met26 (a mixture of M3 and M9), Met22 (a mixture of M1 and Met22-2), Met15 (a mixture of Met15-1 and Met15-2), M7, and Met19 accounted for 4.7%, 2.5%, 1.7%, 1.4%, and 1.1% of the dose, respectively. The amounts of the other metabolites were minor, each accounting for less than 1.0% of the dose.

Structural Analysis of Metabolites. Lemborexant was metabolized to various metabolites via multiple pathways, and a total of 41 metabolites were detected in plasma, urine, and feces collected from subjects receiving a single oral administration of [^{14}C]lemborexant. Of the metabolites detected, the chemical structures of 33 metabolites were identified by comparing retention times on chromatograms and mass spectra of authentic standards and glucuronide conjugates enzymatically generated in vitro or elucidated based on mass fragmentation patterns. The proposed metabolic pathways of lemborexant in humans are shown in Fig. 3. The measured accurate mass and characteristic fragment ions of the metabolites are summarized in Supplemental Table 1. The rationale for the structural elucidation is described in Supplemental Data.

Lemborexant underwent oxidation as the primary metabolism, and was converted to multiple mono-oxidized metabolites. Then, some of the mono-oxidized metabolites were further oxidized to dioxidized metabolites or the carboxylated form, or they were subjected to conjugation with glucuronic acid or sulfuric acid. Amide hydrolysis was also observed as a minor metabolic pathway. Although M17 (glucuronide of M5) was detected in urine, M5 itself was not detected in biologic samples, presumably because of the limited amount in the samples.

Binding Affinity to Human OX1R and OX2R. The affinities of M4, M9, and M10 for human OX1R and OX2R were determined by receptor binding assay. IC_{50} values against human OX1R and OX2R were 11.7 $\pm$ 1.7 and 3.8 $\pm$ 1.1 nmol/l for M4, 18.6 $\pm$ 1.3 and 4.7 $\pm$ 1.5 nmol/l for M9, and 4.2 $\pm$ 1.2 and 2.9 $\pm$ 1.5 nmol/l for M10, respectively. M4, M9, and M10 showed binding affinities that were comparable to those of lemborexant (IC_{50}: 6.1 nmol/L for OX1R and 2.6 nmol/L for OX2R; Beuckmann et al., 2017).
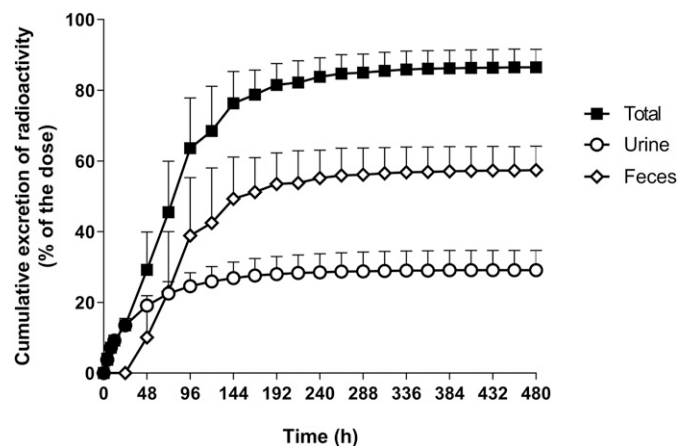

Fig. 2. Cumulative excretion of radioactivity recovered in urine and feces after a single oral administration of [^{14}C]lemborexant at 10 mg (100 μCi) to healthy male subjects. Each point represents the mean + S.D. of eight subjects.

TABLE 2

Relative exposures of lemborexant and its metabolites in AUC-pooled plasma

Individual plasma samples from eight subjects were mixed at equal volume, and a single AUC-pooled plasma sample was prepared from pooled samples collected from 0 to 96 h postdose.

Analyte	M No.	Total Drug-Related Exposure
		%
Met1	—	1.1
Met2	—	1.2
Met3	—	1.6
Met5	—	2.8
Met7	—	3.2
Met8	—	2.2
Met11-2	—	2.0
Met12	M18	6.0
Met16-2	M13	1.6
Met17	M20	1.5
Met18	—	1.4
Met21[a]	M11[b], M14[b]	3.0
Met23	M15	2.6
Met24-1	M12	3.1
Met24-2	M4	6.3
Met26-2	M9	6.6
Met27	M10	12.5
Lemborexant	—	26.5

—, not applicable.
[a]Met21 was a mixture of Met21-1 and Met21-2.
[b]Met21-1 and Met21-2 were identified as M11 and M14.

TABLE 3

Percentages of lemborexant and its metabolites recovered in excreta after a single oral dose of [14C]lemborexant

Urine samples at 0–120 h and fecal samples at 0–264 h postdose were used. Each value represents the mean ± S.D. of eight subjects.

Analyte	M No.	Dose		
		Urine	Feces	Total
		%		
Met4	—	0.5 ± 0.4	ND	0.5 ± 0.4
Met5	—	0.7 ± 0.4	ND	0.7 ± 0.4
Met6	M23	0.5 ± 0.4	ND	0.5 ± 0.4
Met7	—	0.2 ± 0.3	ND	0.2 ± 0.3
Met9[a]	M16[b], M22[b]	1.7 ± 0.4	ND	1.7 ± 0.4
Met10	—	ND	0.3 ± 0.4	0.3 ± 0.4
Met11[c]	M17[d]	0.6 ± 0.3	ND	0.6 ± 0.3
Met12	M18	11.0 ± 2.5	ND	11.0 ± 2.5
Met13	M24	0.9 ± 0.2	ND	0.9 ± 0.2
Met14[e]	—	ND	0.8 ± 0.5	0.8 ± 0.5
Met15[f]	—	ND	1.7 ± 0.4	1.7 ± 0.4
Met16[g]	M13[h]	0.9 ± 0.2	ND	0.9 ± 0.2
Met17	M20	0.5 ± 0.4	ND	0.5 ± 0.4
Met19	—	ND	1.1 ± 0.4	1.1 ± 0.4
Met20	M21	1.4 ± 0.7	ND	1.4 ± 0.7
Met21[i]	M11[j], M14[j]	0.8 ± 0.3	ND	0.8 ± 0.3
Met22[k]	M1[l]	ND	2.5 ± 0.7	2.5 ± 0.7
Met24[m]	M12[n], M4[n]	4.0 ± 1.3	12.0 ± 2.1	16.0 ± 1.8
Met25	M7	ND	1.4 ± 0.3	1.4 ± 0.3
Met26[o]	M3[p], M9[p]	ND	4.7 ± 1.8	4.7 ± 1.8
Met28	M8	ND	0.7 ± 0.5	0.7 ± 0.5
Lemborexant + Met29[q]	—	ND	13.0 ± 5.3	13.0 ± 5.3

—, not applicable; ND, below the lower limit of detection.
[a]Met9 was a mixture of Met9-1, Met9-2, Met9-3, and Met9-4.
[b]Met9-1 and Met9-4 were identified as M16 and M22, respectively.
[c]Met11 was a mixture of Met11-1, Met11-2, and Met11-3.
[d]Met11-1 was identified as M17.
[e]Met14 was a mixture of Met14-1 and Met14-2
[f]Met15 was a mixture of Met15-1 and Met15-2.
[g]Met16 was a mixture of Met16-1 and Met16-2.
[h]Met16-2 was identified as M13.
[i]Met21 was a mixture of Met21-1 and Met21-2.
[j]Met21-1 and Met21-2 were identified as M11 and M14, respectively.
[k]Met22 was a mixture of Met22-1 and Met22-2.
[l]Met22-1 was identified as M1.
[m]Met24 was a mixture of Met24-1 and Met24-2. Met24-2 was not detected in feces.
[n]Met24-1 and Met24-2 were identified as M12 and M4, respectively.
[o]Met26 was a mixture of Met26-1 and Met26-2.
[p]Met26-1 and Met26-2 were identified as M3 and M9, respectively.
[q]Met29 was eluted as a mixture with lemborexant.

P-gp and BCRP Transport. Lemborexant showed high permeability in LLC-PK1 and Madin-Darby Canine Kidney II cells, with a P_{app} of $28–32 \times 10^{-6}$ cm/s. CFR values of lemborexant in the absence of a typical inhibitor were 1.47 for P-gp and 1.28 for BCRP (Table 4). Verapamil, a typical inhibitor of P-gp, showed minimal inhibitory effect on transcellular transport of lemborexant via P-gp, resulting in a slightly lower CFR value (1.16) than that in the absence of verapamil. In contrast, Ko143, a typical inhibitor of BCRP, did not affect the CFR value of lemborexant (1.21). These results indicated that lemborexant is a poor P-gp substrate and is not a substrate of BCRP. M4, M9, and M10 showed relatively high permeability in the cells (P_{app}: $9.6–29 \times 10^{-6}$ cm/s). The CFR values of M4, M9, and M10 for P-gp were 16.3, 2.86, and 4.41, respectively, and these values were decreased substantially in the presence of verapamil. The CFR values of M4, M9, and M10 for BCRP were 1.42 or less, and they were comparable in the absence and presence of Ko143. Based on these results, it was concluded that M4, M9, and M10 are substrates of P-gp but not of BCRP.

In Vitro Plasma Protein Binding. Lemborexant showed relatively high binding to human plasma proteins (87.4%–88.7%). The plasma protein bindings of M4, M9, and M10 were 74.3%–74.4%, 85.3%–86.2%, and 91.5%–92.0%, respectively. No concentration dependence in the plasma protein binding of lemborexant and its metabolites was observed at the concentration range of 100–1000 ng/ml.

Exposure Comparison of Circulating Metabolites between Humans and Animals. Table 5 summarizes the plasma exposure of lemborexant and its metabolites (M4, M9, and M10) after multiple oral administrations of lemborexant in humans and animals. In humans, the $AUC_{(0–24\ h)}$ of lemborexant, M4, M9, and M10 after multiple oral administration of lemborexant was almost comparable to the $AUC_{(0–inf)}$ after single oral administration of [14C]lemborexant (Table 1). Considering these results and the terminal elimination half-lives of lemborexant and its metabolites, a 14-day multiple-dosing regimen in humans would likely be sufficient for comparing exposures at steady state between humans and animals. In rats and monkeys, the $AUC_{(0–24\ h)}$ of lemborexant, M4, M9, and M10 was increased dose-dependently in all groups, except in male monkeys administered at 1000 mg/kg. In rats, there was a sex difference in plasma exposure: females generally showed higher exposures than males, leading to differences in dose levels tested in nonclinical toxicology studies. Plasma exposures of M4, M9, and M10 in rats administered ≥30, ≥10, and 1000 mg/kg lemborexant, respectively, were higher than those at steady state in humans. In monkeys, all dose groups showed higher plasma exposures of the metabolites compared with those at steady state in humans.

Discussion

The aim of the present study was to investigate the disposition and metabolism of [14C]lemborexant in healthy human subjects. In addition, in vitro assessments and exposure comparisons for the circulating metabolites with a relatively high exposure in humans were conducted to evaluate the characteristics of the metabolites from the perspectives of pharmacological activity and safety.

After a single oral administration, [14C]lemborexant was rapidly absorbed, and plasma concentrations of radioactivity peaked at 1 hour postdose. Radioactivity in plasma was eliminated with a terminal elimination half-life of 43.6 hours, and it was excreted mainly into feces, with a mean cumulative recovery of 86.5% of the dose from excreta within 20 days. The sum of the $AUC_{(0–inf)}$ values for lemborexant, M4, M9, and M10 determined by LC-MS/MS accounted
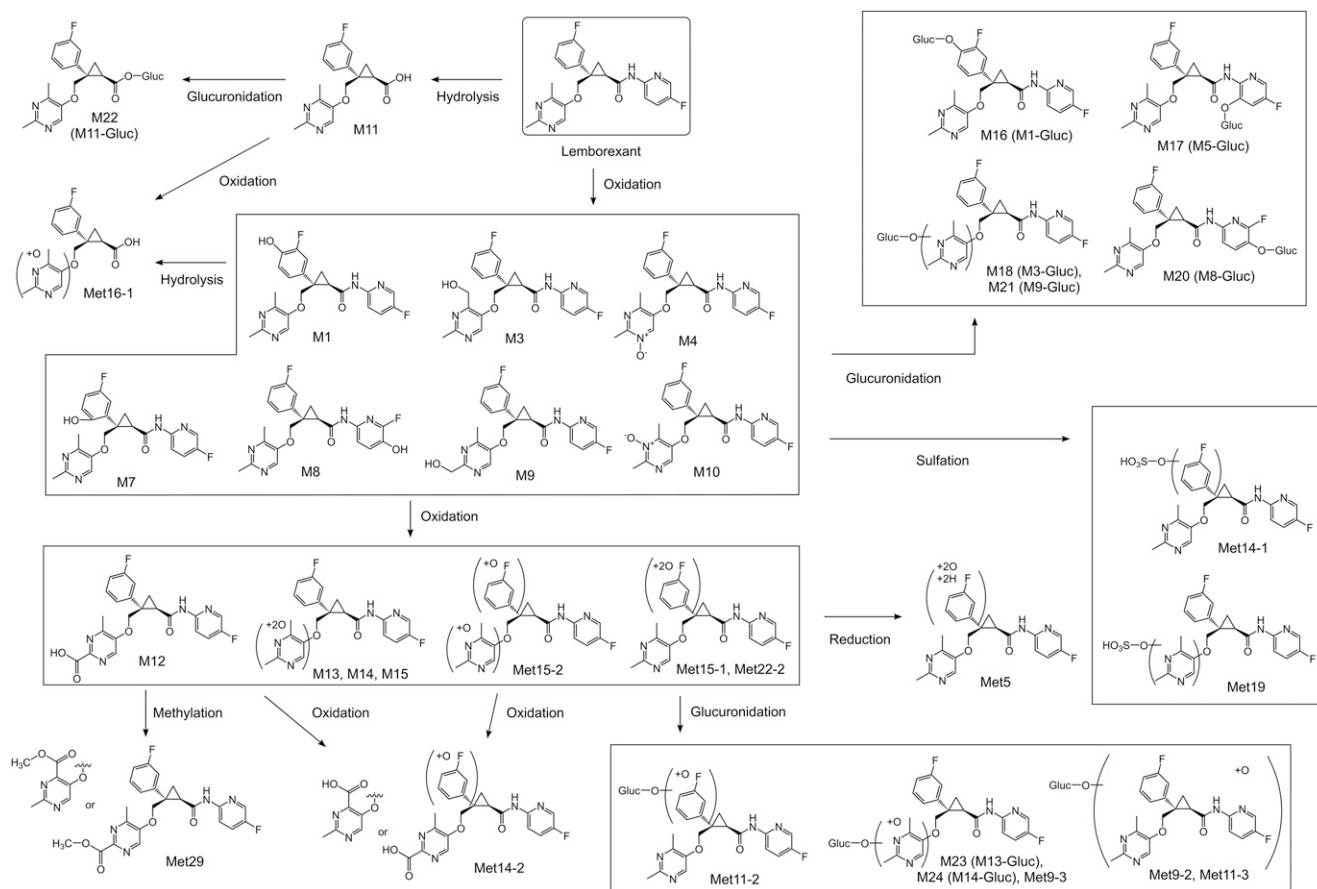
Fig. 3. Proposed metabolic pathways of lemborexant in humans. Gluc, glucuronide.

for approximately 50% of the $AUC_{(0-inf)}$ for radioactivity (Table 1), suggesting that other metabolites existed in plasma. This result is consistent with the outcomes of the metabolic profiling based on the radiochromatography with the AUC-pooling method (Table 2), and the levels of all metabolites other than M4, M9, and M10 were low (each ≤6.0% of total drug-related exposure). Also, the relative exposures of lemborexant, M4, M9, and M10 determined in the metabolic profiling were comparable to those determined by LC-MS/MS, indicating that the AUC-pooled plasma sample prepared by the Hamilton method accurately reflected the mean AUC value.

After oral administration, unchanged lemborexant was not detected in urine but was found as the major radioactive component in feces (approximately 13.0% of the dose; Table 3). In rats and monkeys, [^{14}C]lemborexant administered in solution was almost completely absorbed, and unchanged lemborexant was not detected in the excreta. In addition, no biliary excretion of unchanged lemborexant was observed in rats (Ueno et al., 2019). Considering that no glucuronide metabolites formed by direct conjugation of lemborexant were observed in humans (Fig. 3), unchanged lemborexant detected in feces can be attributed to the unabsorbed fraction of the administered [^{14}C]lemborexant. Lemborexant showed relatively high membrane permeability in vitro. It should be noted that the solubility of lemborexant is low and pH-dependent, with delayed dissolution in weak acid or neutral solutions ((Landry et al., 2020)). Unlike the case with animals that were administered predissolved [^{14}C]lemborexant, its low solubility might be one possibility for incomplete absorption in humans. Therefore, as found in rats and monkeys, in humans, excretion of lemborexant into feces after absorption is minor, and the main elimination pathway of lemborexant is metabolism.

Metabolic profiling demonstrated that lemborexant undergoes metabolism via multiple and diverse pathways. Considering the relative amounts of the metabolites in the excreta, the major metabolic pathways of lemborexant in humans are oxidation of the dimethylpyrimidine moiety of lemborexant and subsequent further oxidation and/or glucuronidation. Although oxidative defluorination was observed as one of the metabolic pathways of lemborexant in rats and monkeys, resulting in the excretion of some defluorinated metabolites in rat and monkey excreta (Ueno et al., 2019), no defluorinated metabolites were observed in human plasma, urine, or feces. M8, which is formed via displacement of fluorine at the fluoropyridine moiety of lemborexant (Supplemental Data), was detected in humans and animals. However, all defluorinated metabolites detected in rats and monkeys were formed via oxidative defluorination at the fluorophenyl moiety of lemborexant (Ueno et al., 2019). In addition, glutathione conjugates were not detected

TABLE 4

Transcellular transport of lemborexant and its metabolites via P-gp and BCRP

Compound	Corrected Flux Ratio			
	P-gp		BCRP	
	−	+	−	+
Lemborexant	1.47	1.16	1.28	1.21
M4	16.3	2.32	1.42	1.21
M9	2.86	1.19	1.04	1.14
M10	4.41	1.22	0.94	0.99

Values represent corrected flux ratios in the absence (−) and presence (+) of a typical inhibitor of P-gp (30 μmol/l verapamil) or BCRP (50 nmol/l Ko143).

TABLE 5

Comparison of plasma exposures of lemborexant and its metabolites between humans and animals

Plasma samples collected after multiple oral administrations of lemborexant for 14 days (humans) and 28 days (rats and monkeys) were used. Each value except for $AUC_{(0-24\ h)}$ in humans represents values of males/females. $AUC_{(0-24\ h)}$ values in humans are expressed as means $\pm$ S.D. of six subjects. Exposure multiple was calculated by dividing $AUC_{(0-24\ h)}$ in animals by that in humans.

Species	Dose	$AUC_{(0-24h)}$				Exposure Multiple		
		Lemborexant	M4	M9	M10	M4	M9	M10
		ng·h/ml						
Human	10 mg/subject	431 ± 226	172 ± 71.4	98.0 ± 54.3	259 ± 110	—	—	—
Rat	10 mg/kg	n.t./584	n.t./2.13	n.t./2100	n.t./1.76	n.t./0.012	n.t./21.4	n.t./0.007
	30 mg/kg	2630/n.t.	238/n.t.	2390/n.t.	9.85/n.t.	1.38/n.t.	24.4/n.t.	0.038/n.t.
	100 mg/kg	16,500/39,100	1600/627	4940/13,600	74.1/204	9.30/3.65	50.4/139	0.286/0.788
	1000 mg/kg	40,000/223,000	2770/12,100	10,100/25,100	259/3070	16.1/70.3	103/256	1.00/11.9
Monkey	10 mg/kg	4090/3820	2290/2020	195/328	353/320	13.3/11.7	1.99/3.35	1.36/1.24
	100 mg/kg	94,000/88,300	33,100/25,200	5660/5950	3650/3210	192/147	57.8/60.7	14.1/12.4
	1000 mg/kg	74,000/162,000	23,000/61,700	2600/13,200	2820/6780	134/359	26.5/135	10.9/26.2

—, not applicable; n.t., not tested.

in humans, although they were found in animals. Considering these data, the metabolic pathway of M8 would not be reactive or related to oxidative defluorination of lemborexant. Like in rats and monkeys, amide hydrolysis was detected as a minor metabolic pathway in humans, presumably resulting in formation of an aromatic amine. It is known that aromatic amines undergo bioactivation and show a carcinogenic potential (Turesky and Le Marchand, 2011). No carcinogenic potentials of lemborexant were confirmed in rat and mouse carcinogenicity assessments (data not shown). Comparison of the metabolic profiles of lemborexant between humans and animals found that all circulating metabolites detected in human plasma, except for M15, were detected in biologic samples in rats or monkeys. However, in a separate study using plasma samples collected from rats and monkeys after multiple oral administrations of lemborexant, M15 was detected by LC-MS/MS analysis in both rats and monkeys (data not shown). Thus, these results indicate no human-specific circulating metabolites. Overall, the metabolic pathways of lemborexant in humans were similar to those in rats and monkeys (Ueno et al., 2019), although oxidative defluorination and glutathione conjugation were not observed in humans.

M10 was detected as the only major circulating metabolite showing ≥10% of total drug-related exposure, but M4, M9, and M18 (glucuronide of M3) were found in human plasma as metabolites showing relatively high plasma exposure (6.0%–6.6% of total drug-related exposure). In general, it is unlikely that glucuronides like M18 exert effects on the central nervous system. Thus, the binding affinities of M4, M9, and M10 to human OX1R and OX2R were assessed in vitro and were found to be comparable to lemborexant. Furthermore, in vitro assessments revealed that lemborexant is a poor substrate of P-gp; that M4, M9, and M10 are good substrates of P-gp; and that the plasma protein bindings of lemborexant and its metabolites in humans are around 70%–90%. Considering that plasma exposure of lemborexant was higher than those of these three metabolites, and brain penetration of these metabolites would likely be less than that of lemborexant in humans because of P-gp transport, lemborexant can be considered to be the main contributor to the pharmacological activity in humans, with the contributions of the metabolites being low.

In long-term nonclinical toxicology studies, the no-observable-adverse-effect level was 30 and 100 mg/kg for female and male rats, respectively, and 10 mg/kg for male and female monkeys (unpublished data). To confirm metabolite exposure in nonclinical toxicology species, plasma exposure of M10, the only major circulating metabolite showing ≥10% of total drug-related exposure, at steady state was determined. The amount of M10 observed in the systemic circulation was limited in rats, but a higher exposure than that in humans was achieved at the

highest dose tested in rats (1000 mg/kg). Meanwhile, plasma exposure of M10 at the lowest dose tested in monkeys (10 mg/kg) exceeded that at the maximum recommended dose in humans (10 mg). M4 and M9 also showed higher exposures at the lowest doses in male rats (30 mg/kg) and in male and female monkeys (10 mg/kg) than those at 10 mg in humans. These results indicated that higher exposure to M4, M9, and M10 was achieved at a no-observable-adverse-effect level in at least one species of the nonclinical toxicological species and that there is no disproportionate metabolite as defined by the International Council for Harmonisation of Technical Requirements for Pharmaceuticals for Human Use M3(R2) and Metabolite in Safety Testing guidance (ICH, 2010; FDA, 2020b). Therefore, no additional toxicology studies are needed from the perspective of metabolite safety.

In summary, the present study investigated the disposition and metabolism of lemborexant in humans. Lemborexant shows rapid absorption after oral administration and undergoes metabolism via multiple pathways, with oxidation as the primary route, and the consequent metabolites are excreted mainly into feces. Although M4, M9, and M10 showed binding affinities to orexin receptors comparable to that of lemborexant, their contributions to the pharmacological effect in humans can be considered to be low because of the lower plasma concentration and brain penetration than the parent drug. Higher exposure to M10, the only major circulating metabolite, in nonclinical toxicology species was confirmed, indicating that there are no disproportionate metabolites in humans, and no additional toxicology studies are needed.

Authorship Contributions

Participated in research design: Ueno, Ishida, Aluri, Suzuki, Beuckmann, Kameyama, Asakura, Kusano.

Conducted experiments: Ueno, Ishida, Suzuki, Kameyama, Asakura.

Contributed new reagents or analytic tools: Ueno, Ishida, Aluri.

Performed data analysis: Ueno, Ishida, Aluri, Suzuki, Kameyama.

Wrote or contributed to the writing of the manuscript: Ueno, Ishida, Beuckmann, Kusano.

References

Beuckmann CT, Suzuki M, Ueno T, Nagaoka K, Arai T, and Higashiyama H (2017) In vitro and in silico characterization of lemborexant (E2006), a novel dual orexin receptor antagonist. *J Pharmacol Exp Ther* **362**:287–295.

Beuckmann CT, Ueno T, Nakagawa M, Suzuki M, and Akasofu S (2019) Preclinical in vivo characterization of lemborexant (E2006), a novel dual orexin receptor antagonist for sleep/wake regulation. *Sleep (Basel)* **42**:zsz076 DOI: 10.1093/sleep/zsz076.

Brisbare-Roch C, Dingemanse J, Koberstein R, Hoever P, Aissaoui H, Flores S, Mueller C, Nayler O, van Gerven J, de Haas SL, et al. (2007) Promotion of sleep by targeting the orexin system in rats, dogs and humans. *Nat Med* **13**:150–155.

Buysse DJ (2013) Insomnia. *JAMA* **309**:706–716.

de Lecea L, Kilduff TS, Peyron C, Gao X, Foye PE, Danielson PE, Fukuhara C, Battenberg EL, Gautvik VT, Bartlett FS II, et al. (1998) The hypocretins: hypothalamus-specific peptides with neuroexcitatory activity. *Proc Natl Acad Sci USA* **95**:322–327.

EMA (2012) *Guideline on the Investigation of Drug Interactions*, European Medicines Agency, Amsterdam.

FDA (2020a) *In Vitro Drug Interaction Studies — Cytochrome P450 Enzyme- and Transporter-Mediated Drug Interactions Guidance for Industry*. U.S. Department of Health and Human Services Food and Drug Administration, Center for Drug Evaluation and Research, Silver Spring, MD.

FDA (2020b) *Safety Testing of Drug Metabolites Guidance for Industry, U.S. Department of Health and Human Services Food and Drug Administration*, Center for Drug Evaluation and Research, Silver Spring, MD.

Hamilton RA, Garnett WR, and Kline BJ (1981) Determination of mean valproic acid serum level by assay of a single pooled sample. *Clin Pharmacol Ther* **29**:408–413.

ICH (2010) *M3(R2) Nonclinical Safety Studies for the Conduct of Human Clinical Trials and Marketing Authorization of Pharmaceuticals*, The International Council for Harmonization of Technical Requirements for Pharmaceuticals for Human Use, Geneva, Switzerland.

Landry I, Aluri J, Hall N, Kumar D, Dayal S, Moline M, and Reyderman L (2020) Effect of gastric acid-reducing agents on the pharmacokinetics and efficacy of lemborexant. *Pharmacol ResPerspect* **8**:e00678.

MHLW (2019) *Guideline on Drug Interaction for Drug Development and Appropriate Provision of Information*, Ministry of Health, Labour and Welfare, Tokyo, Japan.

Morin CM, LeBlanc M, Bélanger L, Ivers H, Mérette C, and Savard J (2011) Prevalence of insomnia and its treatment in Canada. *Can J Psychiatry* **56**:540–548.

Murphy P, Moline M, Mayleben D, Rosenberg R, Zammit G, Pinner K, Dhadda S, Hong Q, Giorgi L, and Satlin A (2017) Lemborexant, A dual orexin receptor antagonist (DORA) for the treatment of insomnia disorder: results from a bayesian, adaptive, randomized, double-blind, placebo-controlled study. *J Clin Sleep Med* **13**:1289–1299.

Rosenberg R, Murphy P, Zammit G, Mayleben D, Kumar D, Dhadda S, Filippov G, LoPresti A, and Moline M (2019) Comparison of lemborexant with placebo and zolpidem tartrate extended release for the treatment of older adults with insomnia disorder: a phase 3 randomized clinical trial. *JAMA Netw Open* **2**:e1918254.

Roth T, Coulouvrat C, Hajak G, Lakoma MD, Sampson NA, Shahly V, Shillington AC, Stephenson JJ, Walsh JK, and Kessler RC (2011) Prevalence and perceived health associated with insomnia based on DSM-IV-TR; international statistical classification of diseases and related health problems, tenth revision; and research diagnostic criteria/international classification of sleep disorders, second edition criteria: results from the America insomnia survey. *Biol Psychiatry* **69**: 592–600.

Sakurai T, Amemiya A, Ishii M, Matsuzaki I, Chemelli RM, Tanaka H, Williams SC, Richarson JA, Kozlowski GP, Wilson S, et al. (1998) Orexins and orexin receptors: a family of hypothalamic neuropeptides and G protein-coupled receptors that regulate feeding behavior. *Cell* **92**: 573–583.

Tozuka Z, Kusuhara H, Nozawa K, Hamabe Y, Ikushima I, Ikeda T, and Sugiyama Y (2010) Microdose study of 14C-acetaminophen with accelerator mass spectrometry to examine pharmacokinetics of parent drug and metabolites in healthy subjects. *Clin Pharmacol Ther* **88**: 824–830.

Turesky RJ and Le Marchand L (2011) Metabolism and biomarkers of heterocyclic aromatic amines in molecular epidemiology studies: lessons learned from aromatic amines. *Chem Res Toxicol* **24**:1169–1214.

Ueno T, Ishida T, and Kusano K (2019) Disposition and metabolism of [^{14}C]lemborexant, a novel dual orexin receptor antagonist, in rats and monkeys. *Xenobiotica* **49**:688–697.

Vermeeren A, Jongen S, Murphy P, Moline M, Filippov G, Pinner K, Perdomo C, Landry I, Majid O, Van Oers ACM, et al. (2019) On-the-road driving performance the morning after bedtime administration of lemborexant in healthy adult and elderly volunteers. *Sleep (Basel)* **42**:zsy260 DOI: 10.1093/sleep/zsy260.

Yoshida Y, Naoe Y, Terauchi T, Ozaki F, Doko T, Takemura A, Tanaka T, Sorimachi K, Beuckmann CT, Suzuki M, et al. (2015) Discovery of (1R,2S)-2-{[(2,4-Dimethylpyrimidin-5-yl) oxy]methyl}-2-(3-fluorophenyl)-N-(5-fluor opyridin-2-yl)cyclopropanecarboxamide (E2006): a potent and efficacious oral orexin receptor antagonist. *J Med Chem* **58**:4648–4664.

Yoshida Y, Terauchi T, Naoe Y, Kazuta Y, Ozaki F, Beuckmann CT, Nakagawa M, Suzuki M, Kushida I, Takenaka O, et al. (2014) Design, synthesis, and structure-activity relationships of a series of novel N-aryl-2-phenylcyclopropanecarboxamide that are potent and orally active orexin receptor antagonists. *Bioorg Med Chem* **22**:6071–6088.

Address correspondence to: Takashi Ueno, Drug Metabolism and Pharmacokinetics, Eisai Co., Ltd., 5-1-3 Tokodai, Tsukuba, Ibaraki 300-2635, Japan. E-mail: t3-ueno@hhc.eisai.co.jp

Supplemental Material

Article Title:

Disposition and Metabolism of [^{14}C]Lemborexant in Healthy Human Subjects and Characterization of Its Circulating Metabolites

Authors:

Takashi Ueno, Tomomi Ishida, Jagadeesh Aluri, Michiyuki Suzuki, Carsten T. Beuckmann, Takaaki Kameyama, Shoji Asakura, Kazutomi Kusano

Journal Title:

Drug Metabolism and Disposition

Manuscript Number:

DMD-AR-2020-000229

Supplemental Data

Rationale for structural characterization of metabolites.

M3, M4, M9, and M10: Each metabolite showed a molecular ion $[M+H]^+$ at m/z 427, 16 Da higher than that of the parent, and fragment ions at m/z 287, 269, 175, 147, 141, 139, and 113. The fragment ion at m/z 141 suggests that lemborexant underwent mono-oxidation at the dimethylpyrimidine moiety. Based on the retention times of authentic standards, structures of M3 and M9 were identified as hydroxylated forms and those of M4 and M10 were identified as *N*-oxide metabolites.

M1 and M7: Both showed the molecular ion $[M+H]^+$ at m/z 427, 16 Da higher than that of the parent, and fragment ions at m/z 303, 285, 191, 163, 139, 125, and 113. The fragment ions at m/z 125 and 113 suggest that lemborexant underwent mono-oxidation at the fluorophenyl moiety. Based on the retention times of authentic standards, the structures of M1 and M7 were identified as hydroxylated forms of lemborexant.

M8: M8 showed a molecular ion $[M+H]^+$ at m/z 427 and fragment ions at m/z 303, 285, 283, 175, 155, 147, 129, and 125. The fragment ion at m/z 129 suggests that lemborexant underwent mono-oxidation at the fluoropyridine moiety. Based on the retention time of an authentic standard, the structure of M8 was identified as a hydroxylated form with a rearrangement of the fluorine on the fluoropyridine moiety, attributed to a mechanism analogous to an NIH-shift.

M13, M14, and M15: Each metabolite showed a molecular ion $[M+H]^+$ at m/z 443, 32 Da higher than that of the parent, and fragment ions at m/z 287, 269, 175, 147, 139, and 113. M13 also showed a fragment ion at m/z 425, and M14 and M15 showed that at m/z 157. The fragment ion at m/z 287 suggests that di-oxidation occurred at the dimethylpyrimidine moiety. Comparing with fragment ions and retention times of authentic standards, M13, M14, and M15 were identified as di-oxidized metabolites.

Met15-1, Met15-2, and Met22-2: Each metabolite showed a molecular ion $[M+H]^+$ at m/z 443, 32 Da higher than that of the parent. Met15-1 and Met22-2 showed key fragment ions at m/z 319 and

207, suggesting that di-oxidation occurred at the fluoropyridine moiety. Met15-2 showed key fragment ions at 303 and 191, suggesting that mono-oxidation occurred at both dimethylpyrimidine and fluorophenyl moieties. Therefore, Met15-1, Met15-2, and Met22-2 were proposed to be di-oxidized metabolites.

M16, M17, M18, M20, and M21: Each metabolite showed a molecular ion [M+H]$^+$ at m/z 603, 192 Da higher than that of the parent. Their fragment ions and retention times were consistent with those of glucuronide conjugates, which were enzymatically generated from hydroxylated metabolites, M1, M5, M3, M8, and M9, respectively, in human liver microsomes fortified with uridine 5′-diphospho-glucuronic acid (UDPGA). Therefore, M16, M17, M18, M20, and M21 were identified as glucuronide conjugates of M1, M5, M3, M8, and M9, respectively.

M23, M24, Met9-2, Met9-3, Met11-2, and Met11-3: Each metabolite showed a molecular ion [M+H]$^+$ at m/z 619, 208 Da higher than that of the parent, suggesting that these metabolites were glucuronide conjugates of di-oxidized metabolites. M23, M24, and Met9-3 showed a key fragment ion at m/z 287, suggesting that di-oxidation and glucuronidation occurred at the dimethylpyrimidine moiety. The fragment ions and retention times of M23 and M24 were consistent with those of glucuronide conjugates that were enzymatically generated from M13 and M14 in human liver microsomes fortified with UDPGA. Thus, the structures of M23 and M24 were identified as glucuronide conjugates of M13 and M14, respectively. Met11-2 showed key fragment ions at m/z 495 and 207, suggesting that di-oxidation and glucuronidation occurred at the fluorophenyl moiety. The structures of Met9-2 and Met11-3 could not be further characterized based on the fragmentation patterns.

Met14-1 and Met19: Each metabolite showed a molecular ion [M+H]$^+$ at m/z 507, 96 Da higher than that of the parent, suggesting that these metabolites were sulfate conjugates of mono-oxidized metabolites. Met14-1 and M19 showed key fragment ions at m/z 191 and 287, respectively, suggesting that mono-oxidation and sulfation occurred at the fluorophenyl and dimethylpyrimidine moieties, respectively.

M11: M11 showed a molecular ion $[M+H]^+$ at m/z 317, 94 Da lower than that of the parent, and fragment ions at m/z 193 and 125. Comparing with fragment ions and retention time of an authentic standard, M11 was identified as a hydrolyzed form of lemborexant.

M22: M22 showed a molecular ion $[M+H]^+$ at m/z 493, 82 Da lower than that of the parent, and fragment ions at m/z 317, 193, and 125. The fragment ions and retention time of M11 were consistent with those of a glucuronide conjugate that was enzymatically generated from M11 in human liver microsomes fortified with UDPGA. Thus, the structure of M11 was identified as a glucuronide conjugate of M11.

Met16-1: Met16-1 showed a molecular ion $[M+H]^+$ at m/z 333, 78 Da lower than that of the parent. Key fragment ions at m/z 193 and 141 suggest that amide hydrolysis and mono-oxidation occurred at the dimethylprimidine moiety. Therefore, Met16-1 was proposed to be a mono-oxidized metabolite of M11.

Met5: Met5 showed a molecular ion $[M+H]^+$ at m/z 445, 34 Da higher than that of the parent. Key fragment ions at m/z 321, 191, and 113 suggest that lemborexant underwent di-oxidation and subsequent reduction at the fluorophenyl moiety. Thus, Met5 was proposed to be a dihydrodiol form of lemborexant.

M12: M12 showed a molecular ion $[M+H]^+$ at m/z 441, 30 Da higher than that of the parent, and fragment ions at m/z 287, 269, 175, 147, 139, and 113. The fragment ion at m/z 287 suggested that lemborexant underwent carboxylation at the dimethylprimidine moiety. Comparing with fragment ions and retention time of an authentic standard, M12 was identified as a carboxylated form of lemborexant.

Met14-2: Met14-2 showed a molecular ion $[M+H]^+$ at m/z 457, 46 Da higher than that of the parent. Key fragment ions at m/z 303 and 191 suggest that fluorophenyl moiety was oxidized and that dimethylpyrimidine moiety was carboxylated. Thus, Met14-2 was proposed to be a carboxylated form of a mono-oxidized metabolite.

Met29: Met29 showed a molecular ion [M+H]$^+$ at *m/z* 455, 44 Da higher than that of the parent. A key fragment ion at *m/z* 169 suggests that dimethylpyrimidine moiety was carboxylated and subsequently methylated. Thus, Met29 was proposed to be a methylated form of a carboxylated lemborexant.

Supplemental Table

Supplemental Table 1. Molecular ions and characteristic fragment ions of lemborexant and metabolites detected in biological samples.

ID	M-No.	Detection	Molecular formula	[M+H]$^+$ Theoretical	[M+H]$^+$ Observed	Δ ppm	Key fragment ions (*m/z*)
Parent	Lemborexant	P, F	$C_{22}H_{21}F_2N_4O_2$	411.16271	411.16318	1.1	287, 269, 175, 147, 139, 125, 113
Met1	—	P	Unknown	—	—	—	—
Met2	—	P	Unknown	—	—	—	—
Met3	—	P	Unknown	—	—	—	—
Met4	—	U	Unknown	—	—	—	—
Met5	—	P, U	$C_{22}H_{23}F_2N_4O_4$	445.16819	445.16757	−1.4	321, 303, 285, 191, 163, 139, 113
Met6	M23 (M13-Gluc)	U	$C_{28}H_{29}F_2N_4O_{10}$	619.18463	619.18472	0.1	443, 425, 287, 269, 175
Met7	—	P, U	Unknown	—	—	—	—
Met8	—	P	Unknown	—	—	—	—
Met9-1	M16 (M1-Gluc)	U	$C_{28}H_{29}F_2N_4O_9$	603.18971	603.18928	−0.7	479, 427, 303, 285, 191, 179, 163, 139, 125, 113
Met9-2	—	U	$C_{28}H_{29}F_2N_4O_{10}$	619.18463	619.18581	1.9	479, 443, 303, 285, 175, 155, 147, 141, 129
Met9-3	—	U	$C_{28}H_{29}F_2N_4O_{10}$	619.18463	619.18581	1.9	443, 287, 269, 175, 157, 147, 139, 113
Met9-4	M22 (M11-Gluc)	U	$C_{23}H_{26}FN_2O_9$	493.16169	493.15977	−3.9	317, 193, 125
Met10	—	F	Unknown	—	—	—	—
Met11-1	M17 (M5-Gluc)	U	$C_{28}H_{29}F_2N_4O_9$	603.18971	603.18958	−0.2	479, 427, 303, 285, 175, 155, 147, 129, 125
Met11-2	—	P, U	$C_{28}H_{29}F_2N_4O_{10}$	619.18463	619.18529	1.1	495, 443, 319, 301, 207, 179, 139, 113

Met11-3	—	U	$C_{28}H_{29}F_2N_4O_{10}$	619.18463	619.18603	2.3	443, 303
Met12	M18 (M3-Gluc)	P, U	$C_{28}H_{29}F_2N_4O_9$	603.18971	603.19153	3.0	427, 287, 269, 175, 147, 141, 139, 113
Met13	M24 (M14-Gluc)	U	$C_{28}H_{29}F_2N_4O_{10}$	619.18463	619.18534	1.1	443, 287, 269, 175, 147, 139, 113
Met14-1	—	F	$C_{22}H_{21}F_2N_4O_6S$	507.11444	507.11472	0.6	427, 303, 285, 191, 163, 139, 113
Met14-2	—	F	$C_{22}H_{19}F_2N_4O_5$	457.13180	457.13227	1.0	303, 285, 191, 179, 163, 139, 113
Met15-1	—	F	$C_{22}H_{21}F_2N_4O_4$	443.15254	443.15281	0.6	319, 301, 207, 179, 139, 125, 113
Met15-2	—	F	$C_{22}H_{21}F_2N_4O_4$	443.15254	443.15281	0.6	303, 285, 191, 179, 163, 139, 113
Met16-1	—	U	$C_{17}H_{18}FN_2O_4$	333.12451	333.12518	2.0	193, 141, 123
Met16-2	M13	P, U	$C_{22}H_{21}F_2N_4O_4$	443.15254	443.15324	1.6	425, 287, 269, 175, 147, 139, 113
Met17	M20 (M8-Gluc)	P, U	$C_{28}H_{29}F_2N_4O_9$	603.18971	603.18953	−0.3	479, 427, 303, 285, 283, 175, 155, 147, 129, 125
Met18	—	P	Unknown	—	—	—	—
Met19	—	F	$C_{22}H_{21}F_2N_4O_6S$	507.11444	507.11559	2.3	427, 287, 269, 175, 147, 139
Met20	M21 (M9-Gluc)	U	$C_{28}H_{29}F_2N_4O_9$	603.18971	603.19066	1.6	427, 287, 269, 175, 147, 139, 113
Met21-1	M11	P, U	$C_{17}H_{18}FN_2O_3$	317.12960	317.12927	−1.0	193, 125
Met21-2	M14	P, U	$C_{22}H_{21}F_2N_4O_4$	443.15254	443.15273	0.4	287, 269, 175, 157, 147, 139, 113
Met22-1	M1	F	$C_{22}H_{21}F_2N_4O_3$	427.15762	427.15805	1.0	303, 285, 191, 179, 163, 139, 125, 113
Met22-2	—	F	$C_{22}H_{21}F_2N_4O_4$	443.15254	443.15287	0.7	425, 319, 301, 207, 179, 139, 113
Met23	M15	P	$C_{22}H_{21}F_2N_4O_4$	443.15254	443.15278	0.5	287, 269, 175, 157, 147, 139, 113
Met24-1	M12	P, U, F	$C_{22}H_{19}F_2N_4O_4$	441.13689	441.13700	0.2	287, 269, 175, 147, 139, 113
Met24-2	M4	P, U	$C_{22}H_{21}F_2N_4O_3$	427.15762	427.15801	0.9	287, 269, 175, 147, 141, 139, 113

Met25	M7	F	$C_{22}H_{21}F_2N_4O_3$	427.15762	427.15817	1.3	303, 285, 191, 163, 139, 125, 113
Met26-1	M3	F	$C_{22}H_{21}F_2N_4O_3$	427.15762	427.15809	1.1	287, 269, 175, 147, 141, 139, 113
Met26-2	M9	P, F	$C_{22}H_{21}F_2N_4O_3$	427.15762	427.15785	0.5	287, 269, 175, 147, 141, 139, 113
Met27	M10	P	$C_{22}H_{21}F_2N_4O_3$	427.15762	427.15820	1.4	287, 269, 175, 147, 141, 139, 113
Met28	M8	F	$C_{22}H_{21}F_2N_4O_3$	427.15762	427.15791	0.7	303, 285, 283, 175, 155, 147, 129, 125
Met29	—	F	$C_{23}H_{21}F_2N_4O_4$	455.15254	455.15273	0.4	287, 269, 175, 169, 147, 139, 113

F: feces, Gluc: glucuronide, P: plasma, U: urine, —: not applicable.

Supplemental Figures

Supplemental Figure 1. Chemical structure of [^{14}C]lemborexant. Asterisk denotes the position of the ^{14}C label.
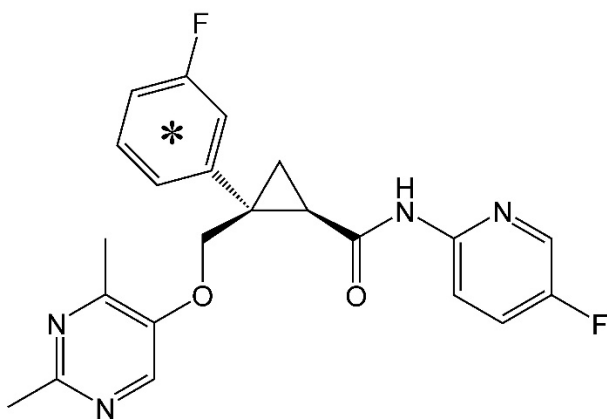
Supplemental Figure 2. Representative HPLC radiochromatograms of metabolites in human plasma, urine, and feces.